ADVANCED MATERIALS

DOI: 10.1002/adma.200602515

Characterizing and Patterning of PDMS-Based Conducting Composites**

By *Xize Niu*, *Suili Peng*, *Liyu Liu*, *Weijia Wen*,* and *Ping Sheng*

In recent years, there has been considerable progress on fabricating microfluidic devices with multiple functionalities, with the goal of attaining lab-on-a-chip[1–3] integration. These efforts have benefited from the development of microfabrication technologies such as soft lithography.[4] In this context the material polydimethylsiloxane (PDMS) has played an important role, not only serving as the stamp for pattern transfer, but also as an unique material in chip fabrication owing to its properties such as transparency, biocompatibility, and good flexibility.[5] Because such microfluidic devices may be constructed using simple manufacturing techniques such as micromolding, they are generally inexpensive to produce. By employing PDMS, micropumps, valves, mixer/reactors, and other components have been integrated into all-in-one chips with complex functionalities, used in chemical reactions, bio-analysis, drug discovery, etc.[2] However, PDMS is a non-conducting polymer, on which patterning metallic structures during the fabrication of microdevices is challenging due to the weak adhesion between the metal and PDMS. Hence, the integration of conducting structures into bulk PDMS has been a critical issue, especially for those applications such as electrokinetic micropumps, microsensors, microheaters, electro-rheological (ER) actuators, etc.,[6–8] which require electrodes for control and signal detection.

Patterning metallic structures is popular in microelectronics, but the metals cannot adhere to PDMS strongly due to the low surface energy of PDMS. Lee et al. reported the transfer and subsequent embedding of thin films of gold patterns into PDMS via chemical adhesion mediated by a silane coupling agent.[9] Lim et al.[10] developed a method of transferring and stacking metal layers onto a PDMS substrate by using serial and selective etching techniques. However, the incompatibility between PDMS and the metal usually caused failures in the fabrication process, especially in the bonding of thin layers. To minimize the difference in material properties, other conductive materials were considered. Gawron et al. reported the embedding of thin carbon fibers into PDMS-based microchips for capillary electrophoresis detection.[11] Carbon black powder is a commonly used material to reinforce the electrical and thermal conductivity and the mechanical strength.[12] PMDS can be turned into a conductive material by the addition of carbon black in a concentration higher than 10 wt % as described by Unger et al.[2] The electrical, rheological, and morphological properties of these materials were studied by Rwei et al.[13] By utilizing a photoresist lift-off technique (using an SU-8 resist), Wong et al.[14] successfully patterned room-temperature vulcanizing (RTV) polymers down to 25 μm feature sizes using a low-resolution mask.

In this paper, we introduce a method of patterning conductive structures by using PDMS-based conducting composites, synthesized by mixing conductive nanometer- to micrometer-sized particles with a PDMS gel.[8] Experimental results indicate that 2D and 3D conducting microstructures can be constructed and integrated into the PDMS bulk material, and such composite microstructures demonstrate excellent conductivity, as well as good mechanical and thermal properties. The advantage of using PDMS-based conducting composites is the ease of bonding and embedding these microstructures into PDMS-based microchips, thereby greatly enhancing their potential functionalities.

The silver or carbon black particle sizes synthesized as described in the Experimental section are about 1–2 μm (silver) and 40–100 nm (carbon black), as can be seen in the insets of Figure 1a and b. The cross-sectional scanning electron

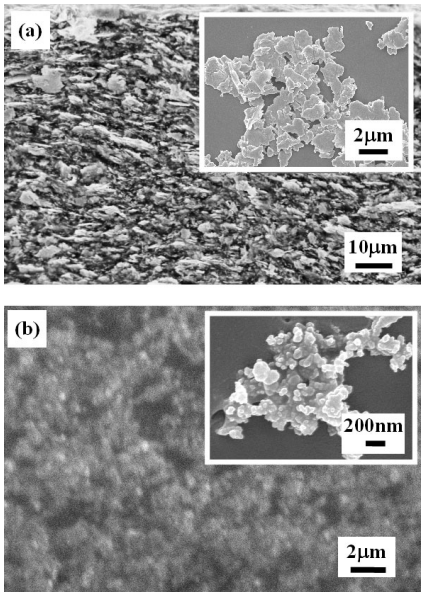

Figure 1. SEM pictures of the cured conductive composite and powders: a) *Ag*+PDMS (84 wt %), b) *C*+PDMS (28 wt %).

[*] Prof. W. J. Wen, Dr. X. Z. Niu, S. L. Peng, L. Y. Liu, Prof. P. Sheng
Department of Physics and Institute of Nano Science and Technology
The Hong Kong University of Science and Technology
Clear Water Bay, Kowloon (Hong Kong)
E-mail: phwen@ust.hk

[**] This work is supported by Hong Kong RGC research project HKUST 604205.

microscopy (SEM) images of the cured composites are shown in Figure 1, wherein the solid particles are seen to be in contact with each other and uniformly distributed in PDMS. From our experience, the silver and carbon black particles were easy to mix with the PDMS gel, perhaps owing to their desirable wetting characteristics.

The conductivities of the two types of composites are shown in Figure 2a, plotted as a function of the concentration of the conducting particles. The threshold concentration for the onset of good conductivity in *Ag*PDMS composites is about 83 wt %. The conductivity σ is seen to increase rapidly beyond the threshold. Similar behavior can be observed for the case of *C*PDMS composites but with a much lower threshold concentration value (ca. 10 wt %), and the conductivity is also much lower (three orders of magnitude smaller than that of the *Ag*PDMS composites). The latter is actually desirable for fabricating microheaters, for example, but unsuitable for those applications where good electrical conduction is required. It should be pointed out here that when the concentration of the solid conducting phase is too high, the composite becomes stiff, easy to break, and difficult to process as the mechanical characteristics no longer resemble those of PDMS. Therefore, obtaining the right concentration is critical for PDMS-based conducting composites.

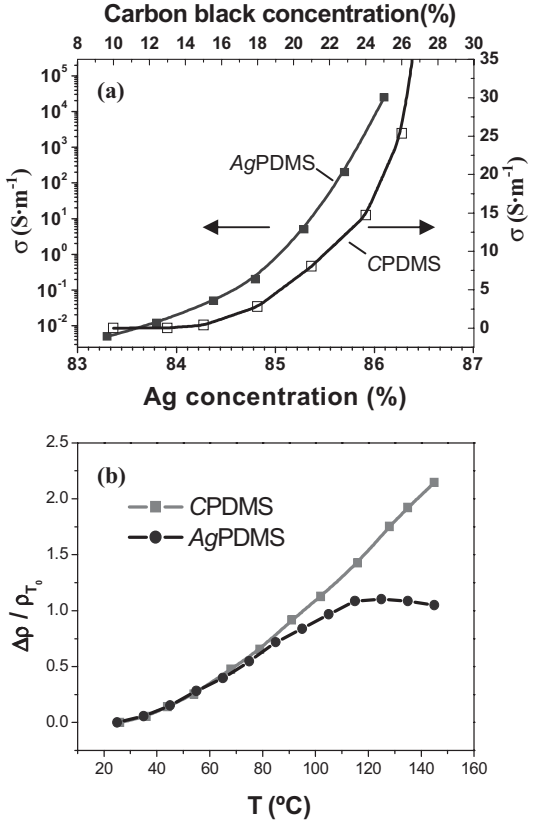

Figure 2. a) Conductivity versus powder weight concentration. b) Variation of resistivity with temperature.

The resistivity, ρ, of well-cured composites exhibits variations with temperature *T*, as shown in Figure 2b. In the temperature range from 25 °C to 150 °C, it is seen that the resistivity of *C*PDMS increases with increasing temperature, while for *Ag*PDMS the resistivity exhibits a peak at about 120 °C and decreases after that. Since these characteristics are reliably repeatable, the temperature variation of the resistivity provides the possibility to design and fabricate thermal sensors by employing these unique thermal characteristics.

The conductivities as a function of strain for two samples are shown in Figure 3a (*C*PDMS) and b (*Ag*PDMS). It is noted that the conductivities for both samples increased monotonically with increasing strain. The reason for this conductivity variation of the sample with strain can be attributed to the change in the conducting particles contact, that is, the carbon-black nanoparticles or silver microparticles have a better chance to contact each other when the samples are stretched, and vice versa. When the strain is released, the conductivity restores to the original value with only a small variation for the *C*PDMS sample. However, the return to the relaxed state for the *Ag*PDMS sample is very slow compared to that for the *C*PDMS sample. It was shown that the former takes more than an hour to restore to its original state. The dynamic characteristics of the sample were also determined, by varying the pull–restore cycle frequency. This was carried out by mounting one end of the sample to a static platform and fixing the other to a mechanical vibrator arm. The peak-to-peak amplitude shown in Figure 3c for the *C*PDMS sample is ca. 1 mm when the vibration frequency is 50 Hz. It should be noted that the waveform as seen in Figure 3c remains discernable even at 200 Hz, implying that these composites can potentially be used as pressure sensors for the detection of dynamic variations of pressure in microchambers or channels. For instance, by using thin PDMS membranes with imbedded conductive lines one could easily detect small pressure changes. Similar dynamic mechanical properties for the *Ag*PDMS sample were found and are shown in Figure 3d.

The procedure to embed one layer of conductive composite into the PDMS elastomer is schematically illustrated in Figure 4a. First a thick layer of photoresist, for instance, AZ 4620, was patterned on a glass substrate using a standard photolithographic technique, for the purpose of forming a mold to pattern the conductive composite. After baking, the mold was treated with a de-molding reagent, tridecafluoro-1,2,2,2-tetrahydrooctyl-1-trichlorosilane. The conducting composite was synthesized by mixing PDMS (Dow Corning 184) and carbon black powder or silver platelets in different concentrations to form *C*PDMS or *Ag*PDMS gels. The gels were then plastered on the mold. Unnecessary portions of the gel were removed from the mold surface (e.g., by using a blade) to ensure that only a clean pattern was left in the mold. After baking for 1 h at 60 °C, the gel was cured into a solid. The photoresist AZ 4620 was then removed by dipping the whole mold substrate into acetone and then ethanol, and subsequent washing with deionized (DI) water. After baking, only PDMS-based conducting composite were left on the substrate,

ADVANCED MATERIALS

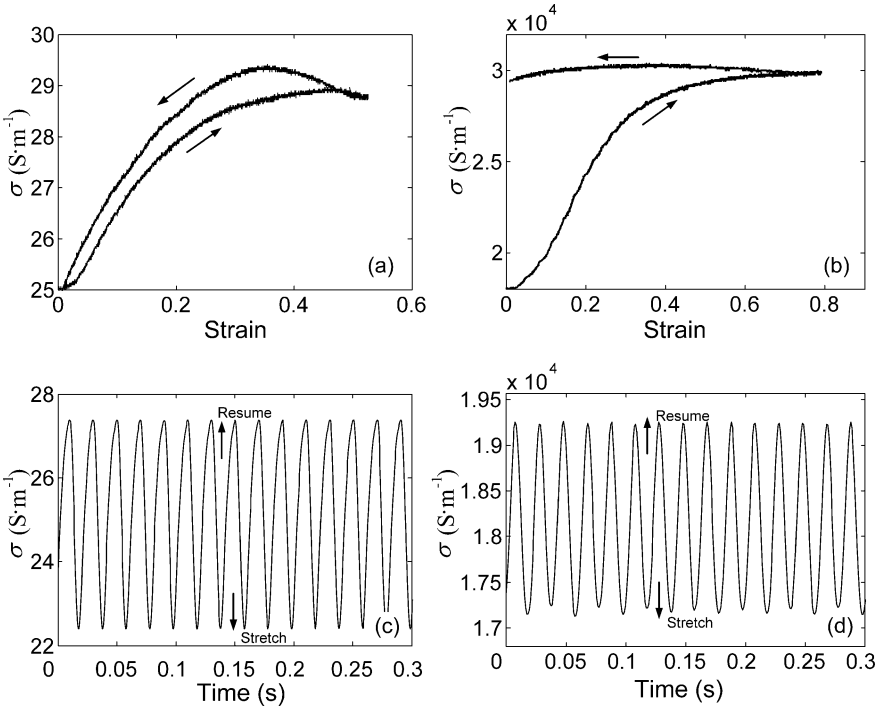

Figure 3. Conductivity variation under stretching of a 26 wt% *C*PDMS strip, 25 mm × 2 mm × 1 mm, and a 86 wt% *Ag*PDMS strip, 25 mm × 1 mm × 1 mm. a,b) Quasi-static stretching and restoring at a rate of 1.5 mm min^{-1} for *C*PDMS (a) and *Ag*PDMS (b). c) Dynamic stretching characteristics of the *C*PDMS sample, peak-to-peak amplitude 1 mm, 50 Hz. d) Dynamic stretching characteristics of the *Ag*PDMS sample, peak-to-peak amplitude 0.5 mm, 50 Hz.

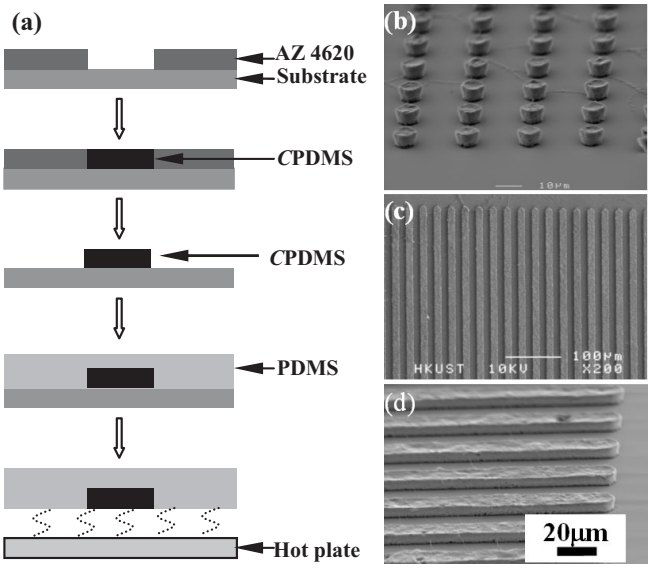

Figure 4. Process flow chart illustrating the patterning of conductive PDMS by soft lithography. a) Micropatterning of the conductive PDMS, b–d) SEM images showing the various fabricated conductive patterns.

shown as step 3 in Figure 4a. The integration or embedding of such conducting micropatterns into a PDMS bulk layer was realized by pouring pure PDMS gel on a substrate whereby the desired microstructure was fully immersed in the PDMS. After spinning to ensure uniformity of the layer, the PDMS sheet with embedded conducting microstructures could easily be peeled off from the substrate (step 4 in Fig. 4a). We have found that the bonding between the fabricated microstructures and bulk PDMS was excellent in all cases. No de-bonding or cracking was found for the fabricated samples after annealing at 150 °C (see the last step in Fig. 4a).

The SEM images of different patterns fabricated with *Ag*PDMS composites are shown in Figure 4b, where one can see that the dimensions of the patterns can range from ten to hundreds of micrometers, indicating the capability to microfabricate conducting devices of different sizes.

Three-dimensional connection of electrical signals is an important issue in integrated microchips, for example, for the transfer of electrical signals among different layers and communication between inner and outer components in multilayered chips. Here we introduce the design and fabrication of 3D microstructures with PDMS-based conducting composites.

For the microstructure depicted in Figure 5a, the fabrication process can be described by a two-mask process as shown in Figure 5b, in which a thin layer (8 μm in thickness) of photoresist (PR) was patterned with the first mask. After being developed, the remaining photoresist structure was hard baked at 150 °C for 30 min to inactivate the photoresist in the next developing process. Then a thick layer of PR (20 μm in demo sample) was coated and patterned to generate "n" shaped cavities on the mold substrate, as depicted in the second panel of Figure 5b. The *Ag*PDMS or *C*PDMS mixture was then plastered into the cavity. After dissolving the two layers of PR with acetone for about 10 min and then rinsing with ethanol and DI water, silane was evaporated onto the sample. A pure PDMS mixture was then poured onto the mold and the sample was placed in vacuum for 20 min to ensure that all cavities were filled with pure PDMS. After curing, the PDMS sheet with conducting patterns can be peeled off from the substrate. With O_2 plasma treatment, the two halves shown in Figure 5c are aligned face to face to bond together under a microscope. The resulting 3D microstructure can be seen in the last right panel of Figure 5c. For such a structure, electrical signals can be transferred along *x* or *y* directions independently without "cross-talk". Figure 5d is a schematic testing approach for the *Ag*PDMS sample indicated above to test the functionalities of the circuit connections with different electronic components. Light-emitting diodes (LEDs) were connected to the lines and light emitting from these LEDs was controlled separately

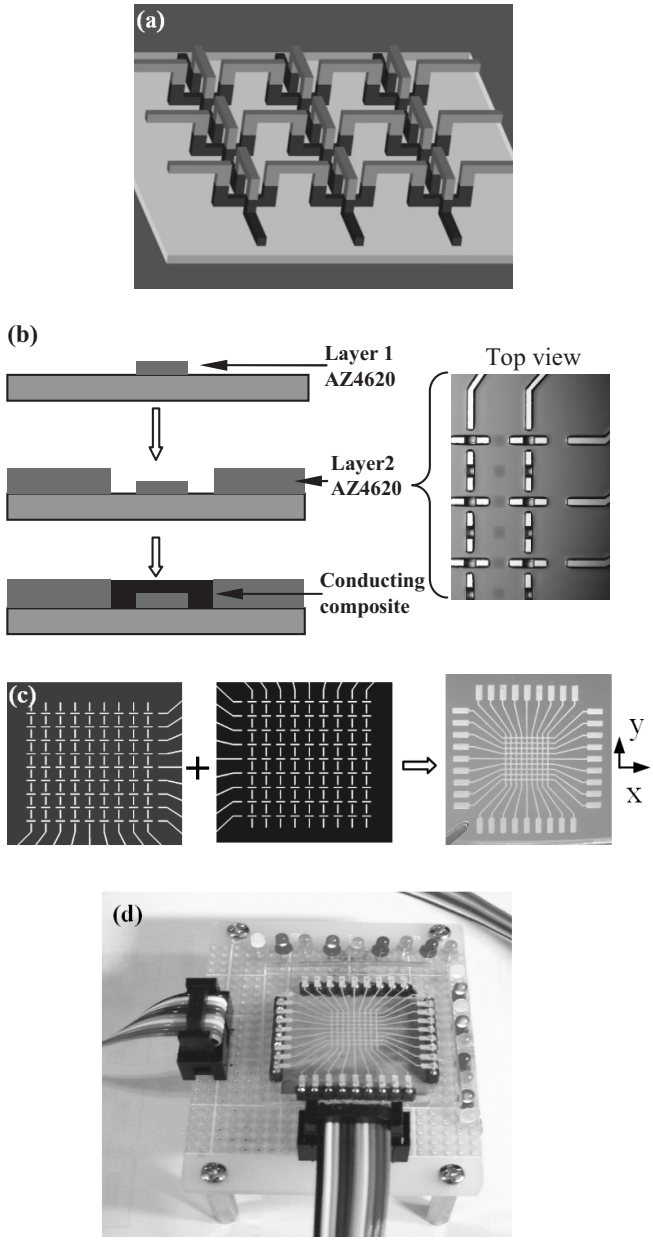

Figure 5. Patterning and bonding of multilayers and 3D conductive PDMS. a) Schematic view of the designed 3D conductive lines. b) Process flow of the microfabrication. c) Reverse bonding of two halves into one plate with jumped lines. d) Testing circuit with LEDs to show the functionality of the bonded plate.

by a Labview program. Since the *Ag*PDMS composite is elastic with good flexibility, the inserted metal pins can be tightly connected to the patches of conducting composite and, therefore, the electric connection is very stable. The testing results indicate that such 3D microstructural wiring can be used for compact connections for electronic parts located on different layers.

This paper demonstrated the fabrication process and application of PDMS-based conducting composites comprising either carbon black nanoparticles or silver microparticles mixed with pure PDMS gel. Experiments show that these composites exhibit good electrical conductivity and mechanical reliability. By using composites of this type we have developed a methodology for constructing planar and 3D microstructures via soft lithography. We also presented a realistic application for 3D microstructures with compact wiring connections. The results obtained are very promising for a variety of applications in microfabricated devices, especially for soft-electronic packaging.

Experimental

Materials: The conducting composites used were PDMS mixed with silver (*Ag*PDMS) (1.2–2.2 μm silver platelet, Unist Business Corp. Shanghai, China) or with carbon (*C*PDMS) (Carbon black, Vulcan XC72-R, Cabot Inc., USA).

Synthesis of PDMS+Ag/C Gel: The silver plate is 1.2–2.2 μm in diameter. Before mixing, it was cleaned with acetone, ethanol, and DI water, then vacuum dried in a freeze-dry system (Labconco). The conductive PDMS mixtures were prepared by mixing the standard components of PDMS with the treated silver powder or carbon black powder directly in a miller to obtain the desired gel.

Characterizing of PDMS Conducting Composites: Two sheets of *Ag*PDMS and *C*PDMS composites were prepared from the conducting gels described above. The conductivities were monitored for increasing solid particle concentration and temperature. Two strips of conducting PDMS samples with dimensions of 25 mm × 2 mm × 1 mm (26 wt % carbon) and 25 mm × 1 mm × 1 mm (86 wt % silver) were prepared for the pulling experiments (MTS, Alliance RT/5). By stretching and restoring the sample with a constant speed of 1.5 mm min^{-1}, the variation of conductivity under strain was determined in situ.

Patterning of PDMS Conducting Composites: Photoresist AZ 4620 was selected for the two layers because it was relatively easy to use for microfabrication. Firstly, a thin layer of AZ 4620 was spin coated at 1200 rpm and then patterned by standard lithography. After being hard baked at 150 °C for 30 min, the areas of alignment marks were covered by tape. The second layer of AZ 4620 was generated by double coating, with 900 rpm for the first coating and baking for 1 min at 95 °C, then 4000 rpm for the second coating and baking for 20 min at 110 °C. The technique does not require the same photoresist to be used and any other photoresist, gel, eutectic alloy, resin, or ammonium salt may also be applied as molding layers assuming they are compactable with the used photolithographic and molding processes. For example, we have tried successfully the integration of microfluidic channels with co-planar parallel electrodes on the channels walls, by using SU-8 as the first molding layer and AZ 4620 as the second one, in the same thickness for the two layers.

Received: November 6, 2006
Revised: December 13, 2006
Published online: August 21, 2007

[1] C. C. Lee, G. D. Sui, A. Elizarov, C. Y. J. Shu, Y. S. Shin, A. N. Dooley, J. Huang, A. Daridon, P. Wyatt, D. Stout, H. C. Kolb, O. N. Witte, N. Satyamurthy, J. R. Heath, M. E. Phelps, S. R. Quake, H. R. Tseng, *Science* **2005**, *310*, 1793.

[2] M. A. Unger, H. P. Chou, T. Thorsen, A. Scherer, S. R. Quake, *Science* **2000**, *288*, 113.

[3] K. A. Shaikh, K. S. Ryu, E. D. Goluch, J. M. Nam, J. W. Liu, S. Thaxton, T. N. Chiesl, A. E. Barron, Y. Lu, C. A. Mirkin, C. Liu, *Proc. Natl. Acad. Sci. USA* **2005**, *102*, 9745.

ADVANCED MATERIALS

[4] Y. N. Xia, G. M. Whitesides, *Annu. Rev. Mater. Sci.* **1998**, *28*, 153.
[5] J. C. McDonald, G. M. Whitesides, *Acc. Chem. Res.* **2002**, *35(7)*, 491.
[6] T. Vilkner, D. Janasek, A. Manz, *Anal. Chem.* **2004**, *76*, 3373.
[7] A. A. Darhuber, J. P. Valentino, J. M. Davis, S. M. Troian, S. Wagner, *Appl. Phys. Lett.* **2003**, *82*, 657.
[8] X. Z. Niu, W. J. Wen, Y. K. Lee, *Appl. Phys. Lett.* **2005**, *87*, 243 501.
[9] K. J. Lee, K. A. Tosser, R. G. Nuzzo, *Adv. Funct. Mater.* **2005**, *15(4)*, 557.
[10] K. S. Lim, W. J. Chang, Y. M. Koo, R. Bashir, *Lab-on-a-Chip* **2006**, *6*, 578.
[11] A. J. Gawron, R. S. Martin, S. M. Lunte, *Electrophoresis* **2001**, *22*, 242.
[12] Q. W. Yuan, A. Kloczkowski, J. E. Mark, M. A. Sharaf. *J. Polym. Sci. Polym. Phys.* **1996**, *34(9)*, 1647.
[13] S. P. Rwei, F. H. Ku, K. C. Cheng, *Colloid Polym. Sci.* **2002**, *280(12)*, 1110.
[14] V. T. S. Wong, A. Huang, C.-M. Ho, *Proc. IEEE MEMS* **2005**, 754.